# Nearness of Subtly Different Digital Images*

Leszek Puzio[1,2] and James F. Peters[1,3]

[1] Computational Intelligence Laboratory
Department of Electrical & Computer Engineering, University of Manitoba
Winnipeg, Manitoba R3T 5V6 Canada
jfpeters@ee.umanitoba.ca
[2] Department of Information Systems and Applications
University of Information Technology and Management
35-225 Rzeszow, ul. H.Sucharskiego 2, Poland
lpuzio@wsiz.rzeszow.pl
[3] School of Mathematics & Computer/Information Sciences,
University of Hyderabad, Central Univ. P.O., Hyderabad 500046, India

**Abstract.** The problem considered in this article is how to measure the nearness or apartness of digital images in cases where it is important to detect subtle changes in the contour, position, and spatial orientation of bounded regions. The solution of this problem results from an application of anisotropic (direction dependent) wavelets and a tolerance near set approach to detecting similarities in pairs of images. A wavelet-based tolerance Nearness Measure (tNM) makes it possible to measure fine-grained differences in shapes in pairs of images. The application of the proposed method focuses on image sequences extracted from hand-finger movement videos. Each image sequence consists of hand-finger movements recorded during rehabilitation exercises. The nearness of pairs of images from such sequences is measured to check the extent that normal hand-finger movement differs from arthritic hand-finger movement. Experimental results of the proposed approach are reported, here. The contribution of this article is an application of an anisotropic wavelet-based tNM in classifying arthritic hand-finger movement images in terms of their degree of nearness to or apartness from normal hand-finger movement images.

**Keywords:** anisotropic wavelets, arthritis, digital image sequence, nearness measure, tolerance near sets.

## 1 Introduction

This paper considers the problem of how to measure the nearness or apartness of digital images in cases where it is important to detect subtle changes in the

* This research was supported by Natural Sciences & Engineering Research Council of Canada (NSERC) grant 185986, Manitoba Center of Excellence Fund (MCEF) grant, Canadian Network of Excellence (CNE), and Canadian Arthritis Network (CAN) grant SRI-BIO-05.

J.T. Yao et al. (Eds): RSKT 2011, LNCS 6954, pp. 543–552, 2011.

contour, position, and spatial orientation of bounded regions. The solution to this problem is given in terms of an anisotropic wavelet-based, tolerance nearness measure in classifying arthritic hand-finger movement images relative to their degree of *nearness* to or *apartness* from normal hand-finger movement images.

In this work, we utilise near set theory informally introduced in 2002 [1] and formally introduced in 2007 [2, 3]. Near sets were inspired by a study of the perceptual resemblance of objects during a collaboration between Z. Pawlak and J.F. Peters [1]. Recent research proves that near set theory can be used effectively to define distance functions that measure the nearness of digital images [4–18]. The anisotropic wavelet-based tolerance nearness measure [9] is based on recent work by C. Henry and J.F. Peters [4, 12, 13]. The contribution of this article is an application of an anisotropic wavelet-based tNM in classifying arthritic hand-finger movement images in terms of their degree of nearness to or apartness from normal hand-finger movement images.

This paper has the following organisation. Sect. 2 gives the basic mathematics underlying the proposed classification method. Sect. 3 briefly presents the nearness measurement method and sample experimental results.

## 2 Preliminaries: Anisotropic Wavelets and Tolerance Nearness Measure

An anisotropic wavelet (*i.e.*, dependent on the direction (angle) that is used to define a wavelet) is constructed in a polar coordinate system as a product of the Hann window function and the Gaussian wavelet [19]. The Hann window function is given in (1).

$$\rho(\alpha) = 0.5(1 - \cos(\alpha)),\ \alpha \in [0, 2\pi), \tag{1}$$

$$\psi(r) = -2r\left(\frac{2}{\pi}\right)^{1/4} e^{-r^2}. \tag{2}$$

An anisotropic wavelet $\psi(\alpha, r)$ is a product of a Hann window $\rho(\alpha)$ and translated by $n_r$ Gaussian wavelet $\psi(r)$ represented in (3). By putting (1) and (2) into (3), we obtain a so-called 'mother wavelet', *i.e.*, a wavelet function (4) that is used to construct a wavelet set. Each wavelet in our set we calculate in (5).

$$\psi(\alpha, r) = \rho(\alpha)\psi(r), \tag{3}$$

$$\psi(\alpha, r) = 0.5(1 - \cos(\alpha))\ (-2r)\left(\frac{2}{\pi}\right)^{1/4} e^{-r^2}, \tag{4}$$

$$\psi_{\mathcal{I}}(\alpha, r) = \tag{5}$$

$$\left(1/\sqrt{2\pi n_r/2^{s_\alpha+1}}\sqrt{2^{-s_r}}\right)\cdot \tag{6}$$

$$\psi\left(2^{s_\alpha}\alpha - \pi(n_\alpha - 1), 2^{-s_r}(r - n_r)\right), \tag{7}$$

$$C_\psi\{f\}(\dots) = \int\int f(\alpha, r)\psi^*_{s_\alpha,s_r,n_\alpha,n_r}(\alpha, r)\, d\alpha\, dr. \tag{8}$$

where $C_\psi\{f\}(\ldots)$ denotes $C_\psi\{f\}(s_\alpha, s_r, n_\alpha, n_r)$, $\psi$ denotes a wavelet with $(\alpha, r)$ a polar coordinates and where $\mathcal{I} = \{s_\alpha, s_r, n_\alpha, n_r\}$ denotes an index set used in (5) to define a wavelet with an angular scale $s_\alpha$, radial scale $s_r$, an angular translation $n_\alpha$ and a radial translation $n_r$. In particular, it is $n_\alpha$ that makes (5) anisotropic, while $n_r$ is a radial distance from the pole (origin of a polar coordinate system).

Perception-based description of an object $x$ in near set theory is in the form of feature vectors $\boldsymbol{\phi(x)}$ containing *probe function* values [7, 14], where

$$\boldsymbol{\phi(x)} = (\phi_1(x), \phi_2(x), \ldots, \phi_i(x), \ldots, \phi_l(x))^T \tag{9}$$

where $\phi_i : O \longrightarrow [0, \infty]$ is a probe function that represents a single object feature. This leads to the notion of a perceptual information system.

**Definition 1. Perceptual information system** [7]
*A* perceptual information system $\langle O, \mathbb{F}\rangle$ *or more concisely, perceptual system is a real-valued, total deterministic information system where O is a non-empty set of* perceptual objects, *while* $\mathbb{F}$ *a countable set of* probe functions.

**Definition 2. Perceptual tolerance relation** [20, 21] *Let* $\langle O, \mathbb{F}\rangle$ *be perceptual system and put* $\varepsilon \in (0, \infty]$. *For every* $\mathcal{B} \subseteq \mathbb{F}$, *the perceptual tolerance relation* $\cong_{\mathcal{B},\varepsilon}$ *is defined as (10).*

$$\cong_{\mathcal{B},\varepsilon} = \{(x, y) \in O \times O \mid \ \phi \in \mathcal{B}, \| \phi(x) - \phi(y) \| \leq \varepsilon\} \tag{10}$$

*where* $\| \cdot \|_2$ *is the* $L_2$ *norm,* $\phi(x) = [\phi_1(x) \ldots \phi_i(x) \ldots \phi_l(x)]^T$ *is a feature vector obtained using all probe functions* $\phi_i \in \mathcal{B}$. *For simplicity, we write* $x \cong_{\mathcal{B}} y$ *instead of* $x \cong_{\mathcal{B},\varepsilon} y$.

Relations with the same formal properties as similarity relations of sensations considered by Poincaré [22] are nowadays, after Zeeman [23], called *tolerance relations.*

A *tolerance* $\tau$ *on a set* $O$ is a relation $\tau \subseteq O \times O$ that is reflexive and symmetric. Transitive tolerance relations are equivalence relations. A set $O$ together with a tolerance $\tau$ is called a *tolerance space* (denoted $\langle O, \tau\rangle$). The useful notion of a tolerance preclass was first introduced by M.J. Schroeder and M.H. Wright [24]. A set $A \subseteq O$ is a $\tau$*-preclass* (or briefly *preclass* when $\tau$ is understood) if and only if for any $x, y \in A$, $(x, y) \in \tau$. The family of all preclasses of a tolerance space is naturally ordered by set inclusion and

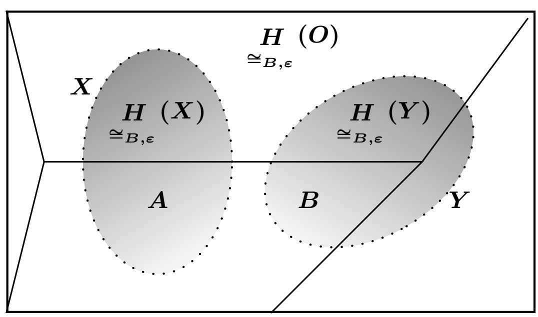


**Fig. 1.** Sample Tolerance Near Sets

preclasses that are maximal with respect to a set inclusion are called *$\tau$-classes* or just *classes*, when $\tau$ is understood. The family of all classes of the space $\langle O, \tau \rangle$ is denoted by $H_\tau(O)$. The family $H_\tau(O)$ is a covering of $O$.

**Definition 3. Tolerance Near Sets** [20, 21]
*Let $\langle O, \mathbb{F} \rangle$ be a perceptual system and let $X, Y \subseteq O$. A set $X$ is perceptually near a $Y$ within the perceptual system $\langle O, \mathbb{F} \rangle$ (*i.e.*, $(X \underline{\underline{\bowtie}}_{\mathbb{F}} Y)$) iff there are such $x \in X$ and $y \in Y$ and there is $\mathcal{B} \subseteq \mathbb{F}$ such that $x \cong_{\mathcal{B},\varepsilon} y$. We than say that $X, Y$ are* perceptually near *each other in the tolerance sense of nearness in Def.2.*

Fig. 1 points to candidate tolerance near sets. Let $O$ denote a set of pixels inside the rectangle. Further, assume $\underset{\cong_{B,\varepsilon}}{\boldsymbol{H}}(\boldsymbol{O})$ denotes the family of all tolerance classes of the space $\langle O, \cong_{B,\varepsilon} \rangle$ determined by the tolerance relation $\cong_{B,\varepsilon}$ in a covering of the nonempty set $O$. Let $X, Y \subset O$ be represented by the shaded ellipses in Fig. 1. In this Figure, tolerance class $A \in \underset{\cong_{B,\varepsilon}}{\boldsymbol{H}}(\boldsymbol{X})$ and tolerance class $B \in \underset{\cong_{B,\varepsilon}}{\boldsymbol{H}}(\boldsymbol{Y})$. For simplicity, let the set of probe functions $B = \{\phi_{gr}\}$, where $\phi_{gr}(o)$ = intensity for pixel $o \in O$. It is apparent from the greylevel intensities in classes $A$ and $B$, that these classes contain pixels with similar descriptions, *i.e.*, pixels with similar intensities. To determine nearness of tolerance spaces, we consider the tolerance nearness measure $tNM$.

**Definition 4. Tolerance Nearness Measure (tNM)** [4]
*The distance $D_{tNM} : \mathcal{P}(O) \times \mathcal{P}(O) :\longrightarrow [0, \infty]$ is defined by*

$$D_{tNM}(X, Y) = \begin{cases} 1 - tNM_{\cong_{\mathcal{B},\varepsilon}}(A, B), & \textit{if } X \textit{ and } Y \textit{ are not empty}, \\ \infty, & \textit{if } X \textit{ or } Y \textit{ is empty}, \end{cases}$$

*where*

$$tNM_{\cong_{\mathcal{B},\varepsilon}}(X, Y) = \left( \sum_{C \in H_{\cong_{\mathcal{B},\varepsilon}}(Z)} |C| \right)^{-1} \cdot \sum_{C \in H_{\cong_{\mathcal{B},\varepsilon}}(Z)} |C| \frac{\min(|C \cap X|, |[C \cap Y|)}{\max(|C \cap X|, |C \cap Y|)}.$$

*For simplicity, $tNM$ is abbreviated $NM$. The details concerning $NM$ are given in [4, 8, 9, 13] and not repeated here.*

Nearness measure values range from 0 to 1 ($tNM(X, Y) = 0$ means that sets $X, Y$ are near (*i.e.*, $X, Y$ have similar descriptions), while $tNM(X, Y) = 1$ means that sets $X, Y$ are far apart (*i.e.*, $X, Y$ have dissimilar descriptions)).

**Example 1. Sample image features extraction using wavelet method**
*We study images resemblance using features obtained using a wavelet-based edge extraction method [25]. This method is based on a anisotropic wavelet [19]. Each edge is described by localization, orientation, wavelet coefficient proportional to edge gradient value, object contour number and contour lengths. Fig. 2 presents example of the use of the wavelet algorithm on an image containing a circle.*

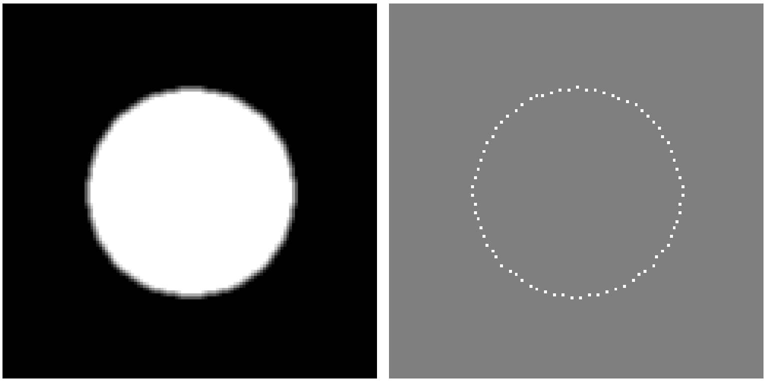

**Fig. 2.** Left: Image with a 'circle' (size 128x128 px). Right: Points where edges were detected using the wavelet algorithm

**Table 1.** Results obtained for 'circle' image in scale $s_r$=1

| # | x | y | orient. [rad] | wav. coef. |
|---|---|---|---|---|
| 0 | 58 | 29 | 4,4 | 0,765 |
| 1 | 61 | 29 | 4,5 | 1,099 |
| 2 | 64 | 28 | -1,6 | 1,169 |
| 3 | 67 | 29 | -1,4 | 1,099 |
| 4 | 70 | 29 | -1,5 | 1,023 |
| 5 | 73 | 30 | -1,2 | 0,998 |
| 6 | 76 | 31 | -1,4 | 1,125 |
| 7 | 79 | 32 | -1,1 | 1,202 |
| 8 | 82 | 33 | -1,0 | 1,140 |
| 9 | 84 | 35 | -1,0 | 1,199 |
| 10 | 87 | 37 | -1,0 | 1,229 |
| 11 | 89 | 39 | -0,8 | 1,218 |
| 12 | 91 | 41 | -0,6 | 1,229 |
| 13 | 93 | 44 | -0,5 | 1,199 |
| 14 | 95 | 47 | -0,6 | 1,211 |
| 15 | 96 | 50 | -0,3 | 0,987 |
| 16 | 97 | 53 | -0,3 | 1,121 |
| 17 | 98 | 56 | -0,2 | 1,123 |
| 18 | 99 | 59 | -0,3 | 1,137 |
| 19 | 100 | 62 | 0,0 | 1,153 |
| 20 | 100 | 65 | 0,0 | 1,169 |
| 21 | 99 | 68 | 0,4 | 0,997 |
| 22 | 99 | 71 | 0,1 | 1,075 |
| 23 | 98 | 74 | 0,4 | 0,834 |
| 24 | 97 | 77 | 0,3 | 1,173 |
| 25 | 96 | 80 | 0,5 | 1,181 |
| 26 | 94 | 82 | 0,6 | 0,888 |
| 27 | 93 | 85 | 0,6 | 0,864 |
| 28 | 91 | 87 | 0,7 | 1,160 |
| 29 | 89 | 89 | 0,8 | 1,228 |
| 30 | 87 | 91 | 1,0 | 1,229 |
| 31 | 84 | 93 | 1,0 | 1,199 |
| 32 | 81 | 95 | 1,0 | 1,207 |
| 33 | 78 | 96 | 1,1 | 1,053 |
| 34 | 75 | 98 | 1,4 | 1,059 |
| 35 | 72 | 98 | 1,4 | 1,124 |
| 36 | 69 | 99 | 1,3 | 1,137 |
| 37 | 66 | 100 | 1,5 | 1,153 |
| 38 | 63 | 100 | 1,6 | 1,169 |
| 39 | 60 | 99 | 1,9 | 0,997 |
| 40 | 57 | 99 | 1,6 | 1,075 |
| 41 | 54 | 98 | 2,0 | 0,866 |
| 42 | 51 | 97 | 1,9 | 1,186 |
| 43 | 48 | 96 | 2,1 | 1,192 |
| 44 | 46 | 94 | 2,2 | 0,888 |
| 45 | 43 | 93 | 2,2 | 0,864 |
| 46 | 41 | 91 | 2,2 | 1,160 |
| 47 | 39 | 89 | 2,4 | 1,228 |
| 48 | 37 | 87 | 2,6 | 1,229 |
| 49 | 35 | 84 | 2,6 | 1,199 |
| 50 | 33 | 81 | 2,5 | 1,211 |
| 51 | 32 | 78 | 2,8 | 0,987 |
| 52 | 31 | 75 | 2,8 | 1,121 |
| 53 | 30 | 72 | 2,9 | 1,123 |
| 54 | 29 | 69 | 2,9 | 1,137 |
| 55 | 28 | 66 | 3,1 | 1,153 |
| 56 | 28 | 63 | 3,1 | 1,169 |
| 57 | 29 | 60 | 3,5 | 0,997 |
| 58 | 29 | 57 | 3,2 | 1,075 |
| 59 | 30 | 54 | 3,6 | 0,834 |
| 60 | 31 | 51 | 3,5 | 1,173 |
| 61 | 32 | 48 | 3,6 | 1,181 |
| 62 | 34 | 46 | 3,7 | 0,888 |
| 63 | 35 | 43 | 3,7 | 0,864 |
| 64 | 37 | 41 | 3,8 | 1,160 |
| 65 | 39 | 39 | 3,9 | 1,228 |
| 66 | 41 | 37 | 4,2 | 1,229 |
| 67 | 44 | 35 | 4,2 | 1,199 |
| 68 | 47 | 33 | 4,1 | 1,207 |
| 69 | 50 | 32 | 4,2 | 1,053 |
| 70 | 53 | 30 | 4,6 | 1,059 |
| 71 | 56 | 30 | 4,5 | 1,124 |

*Table 1 contains sample wavelet algorithm results for Figure 2. The algorithm reveals that one contour containing 72 edges was extracted. Each edge has its order number, position x,y, spatial orientation in radian, and wavelet coefficient.*

## 3 Anisotropic Wavelet-Based Tolerance Nearness

This section introduces an an application of the anisotropic wavelet algorithm from [25] considered in the context of tolerance near sets.

### 3.1 Image Comparison Methodology

**Fig. 3.** Single images from two video sequences, left: normal hand, right: rheumatic hand

**Algorithm 1**: Algorithm steps

**Input** : $Img1$,$Img2$ (pair of images), $s_r$ (wavelet algorithm scale), $\varepsilon$ (tolerance).
**Output**: $NM$ (Nearness Measure value).

1 Initialize algorithm parameters:
(1.1) $s_r \leftarrow$ wavelet scale value;
(1.2) $\varepsilon \leftarrow$ Nearness Measure tolerance value;
2 Extract $Img1, Img2$ features using anisotropic wavelets from Sect. 2:
(2.1) $Feat1 \leftarrow WavAlg(s_r, Img1)$;
(2.2) $Feat2 \leftarrow WavAlg(s_r, Img2)$;
3 Obtain edge positions from images features:
(3.1) $X \leftarrow Feat1(x, y)$;
(3.2) $Y \leftarrow Feat2(x, y)$;
Compute $tNM$ from Def. 4:
$NM \leftarrow tNM_{\cong_{\mathcal{B},\varepsilon}}(X, Y)$;

A method that combines the original anisotropic wavelet algorithm [25] and tolerance nearness distance tNM is summarised in Alg. 1. In this work, hand-finger movement video recording are made during rehabilitation exercise. Sequences of images are extracted from those videos. For every image in an image sequence, we extract features such us edge localization, edge spatial orientation, wavelet coefficient proportional to edge gradient value, objects contour number and contour lengths using a wavelet algorithm. Those features was utilized to nearness measures evaluation of two images from sequence, *i.e.*, first image with second, second with third, and so on.

### 3.2 Experimental Results

To measure the nearness of a pair of digital images, we utilize the tNM measure from Def. 4. Image features are obtained using the wavelet algorithm from Sect. 2 and [25]. NM was based on edge localization, wavelet coefficient value and object contour length features.

As was expected decreasing $\varepsilon$ results in NM values decreasing. This is illustrated in Figure 4, with the X axis marked a succession of pairs of images from video sequence. On the Y axis, tNM values are given for pairs of images. Each plot consists of four data series, because image features was extracted for a different scale parameter of the wavelet algorithm.

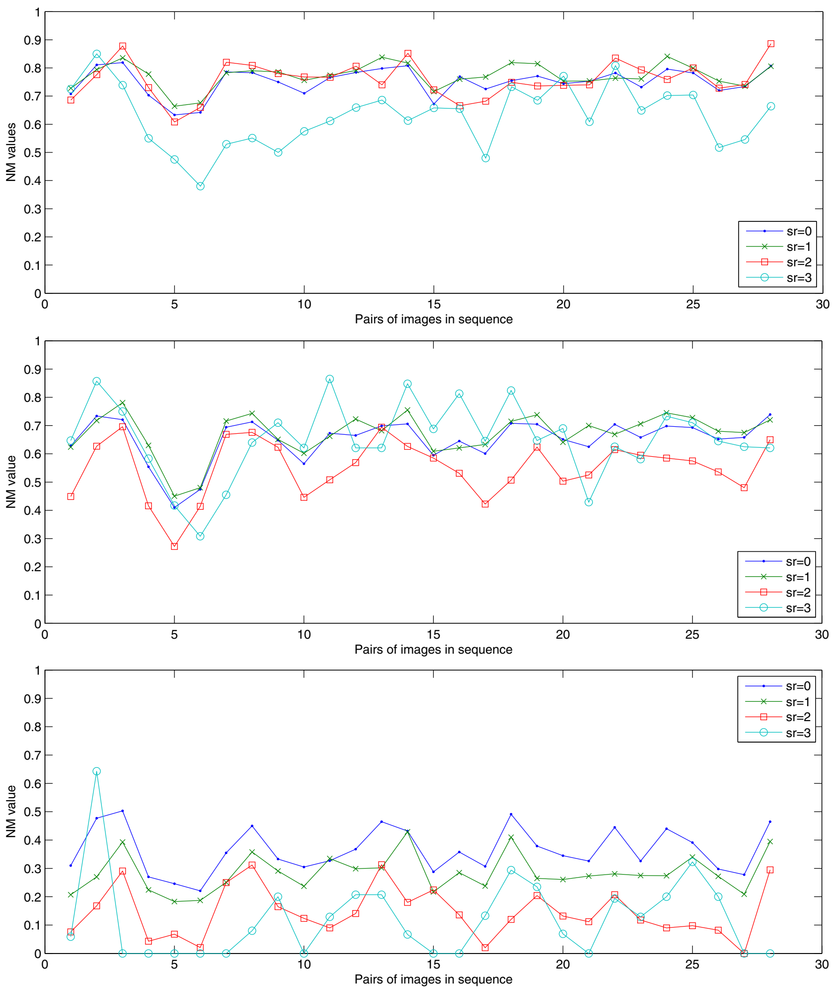


**Fig. 4.** NM values for e=0.1, e=0.05 i e=0.01 values

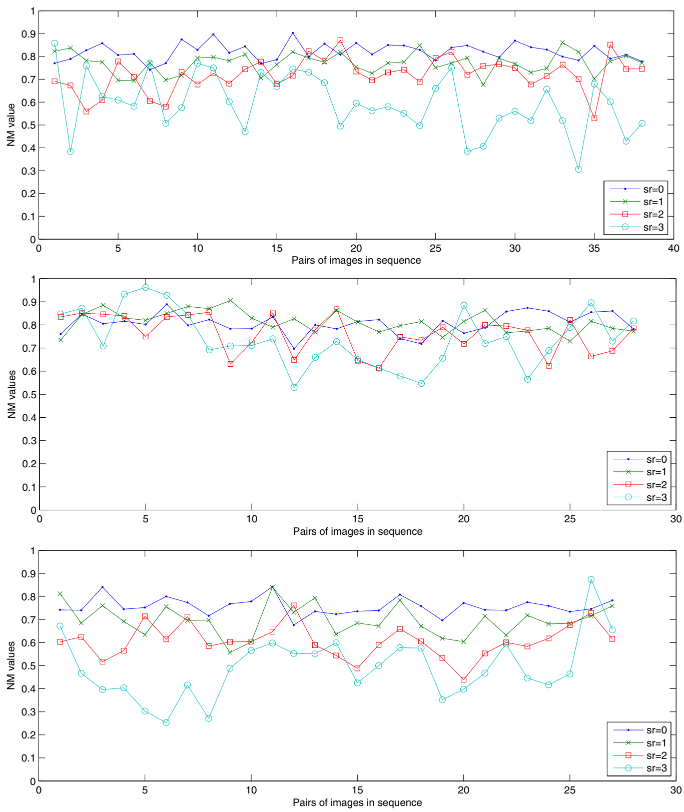


**Fig. 5.** NM values obtained using spatial orientation feature for three different sequences (a) normal 1, (b) normal 2, (c) arthritic

We conclude by our research, that applying such image features as edge spatial orientation, contour number, or contour length to NM calculation results in small difference in obtained NM values for given images sequences. Figure 5 illustrates this, where for three images sequences with calculated NM values that are on almost the same level.

In sum, we conclude that the best distinction between normal and arthritic hand-finger sequences with NM based on edge localization as a image feature occurs with tolerance value 1%.

Figure 6 presents nearness measures values for hand-finger image pairs. It is clear that NM values for normal hand sequences are two times bigger (on average) than arthritic hand sequences. This suggests that this the tNM distance function is able to distinguish between normal and arthritic hand-finger movements.

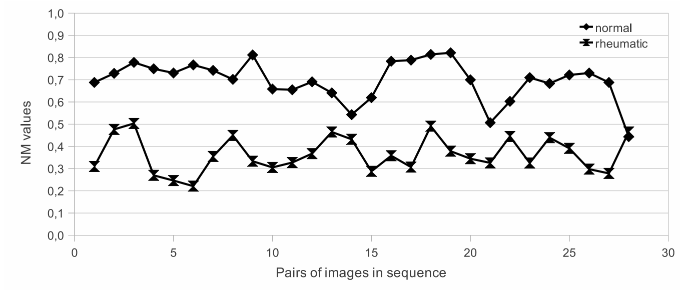


**Fig. 6.** NM of normal and arthritic hand sequences

## 4 Conclusion

This paper presents a number of research results, namely,

(result.i) We are able to apply near sets theory and the tNM measure with wavelets in image analysis.

(result.ii) The Puzio-Walczak wavelet algorithm has utility in image edge extraction for a number of parameters: position, spatial orientation, number and length of objects contours.

(result.iii) It is possible to distinguish between normal and arthritic hand-finger movements using the tNM distance function based on edge position with $\varepsilon = 1\%$.

Future work will include further work on a family of wavelet-based nearness distance functions and classification of images containing subtly different shapes.

## References

1. Pawlak, Z., Peters, J.: How near. Systemy Wspomagania Decyzji I, 57 (2002)
2. Peters, J.: Near sets. Special theory about nearness of objects. Fund. Inform. 75(1-4), 407–433 (2007)
3. Peters, J.: Near sets. General theory about nearness of objects. Applied Math. Sci. 1(53), 2609–2629 (2007)
4. Henry, C.: Near Sets: Theory and Applications, Ph.D. dissertation, supervisor: J.F. Peters. PhD thesis, Department of Electrical & Computer Engineering (2010)
5. Henry, C., Peters, J.: Arthritic hand-finger movement similarity measurements: Tolerance near set approach. Comp. & Math. Methods in Medicine 2011, 1–14 (2011), doi:10.1155/2011/569898
6. Pal, S., Peters, J.: Rough Fuzzy Image Analysis. In: Foundations and Methodologies, Chapman & Hall/CRC Press Mathematical & Computational Imaging Sciences, London, UK (2010)
7. Peters, J., Wasilewski, P.: Foundations of near sets. Info. Sci. 179, 3091–3109 (2009)
8. Hassanien, A., Abraham, A., Peters, J., Schaefer, G., Henry, C.: Rough sets and near sets in medical imaging: A review. IEEE Trans. Info. Tech. in Biomedicine 13(6), 955–968 (2009), doi:10.1109/TITB.2009.2017017

9. Peters, J., Puzio, L.: Image analysis with anisotropic wavelet-based nearness measures. Int. J. Computational Intell. Sys. 22(3), 168–183 (2009)
10. Henry, C., Peters, J.F.: Near set evaluation and recognition (near) system. Technical report, Computational Intelligence Laboratory, University of Manitoba, UM CI Laboratory Technical Report No. TR-2009-015 (2009)
11. Ramanna, S., Meghdadi, A.: Measuring resemblances between swarm behaviours: A perceptual tolerance near set approach. Fundamenta Informaticae 95(4), 533–552 (2009)
12. Henry, C., Peters, J.: Perceptual image analysis. Int. J. Bio-Inspired Comput. 2(3-4), 271–181 (2010), `http://inderscience.metapress.com/link.asp?id=r5w2662q8m18rg23`
13. Henry, C., Peters, J.: Perception-based image classification. Int. J. Intell. Comput. Cybern. 3(3), 410–430 (2010), `http://www.emeraldinsight.com/1756-378X.htm`
14. Peters, J.: Metric spaces for near sets. Ap. Math. Sci. 5(2), 73–78 (2011)
15. Peters, J., Naimpally, S.: Approach spaces for near filters. Gen. Math. Notes 2(1), 159–164 (2011)
16. Peters, J., Tiwari, S.: Approach merotopies and near filters. Gen. Math. Notes 2(2), 1–15 (2011)
17. Henry, C., Peters, J.: Near sets. Wikipedia (2011), `http://en.wikipedia.org/wiki/Near_sets`
18. Peters, J.: Visual perception in image analysis. Digital image content via tolernace near sets. Innovations in Intell. Image Anal. 339, 105–125 (2011), doi:10.1007/978-3-642-17934-16
19. Puzio, L., Walczak, A.: 2-d wavelet with position controlled resolution. In: SPIE Medical Imaging, vol. 5959, p. 59590S (2005), doi = 10.2478/s11772-007-0040-6
20. Peters, J.F.: Tolerance near sets and image correspondence. Int. J. of Bio-Inspired Comput. 1(4), 239–245 (2009)
21. Peters, J.F.: Corrigenda and addenda: Tolerance near sets and image correspondence. Int. J. of Bio-Inspired Comput. 2(5), 310–318 (2010)
22. Poincaré, J.: Dernières pensées, trans. by J.W. Bolduc as Mathematics and Science: Last Essays. Flammarion & Kessinger Pub., Paris & NY (1913)
23. Zeeman, E.: The topology of the brain and visual perception. In: Fort Jr., M.K. (ed.) Topology of 3-Manifolds and Related Topics, University of Georgia Institute Conference Proceedings, pp. 240–256. Prentice-Hall, Inc., Englewood Cliffs (1962)
24. Schroeder, M., Wright, M.: Tolerance and weak tolerance relations. Journal of Combinatorial Mathematics and Combinatorial Computing 11, 123–160 (1992)
25. Puzio, L., Walczak, A.: Adaptive edge detection method for images. Opto-Electronics Review 16(1), 60–67 (2008)